JMEPEG (2005) 14:307-314
DOI: 10.1361/10599490523904

1059-9495/$19.00

Analysis of Hard-Facing Appearance of Specific Powdered Superalloys for PTA-Coating Processes

Ming-Der Jean, Shu-Yi Tu, and Jen-Ting Wang

(Submitted July 29, 2004; in revised form March 24, 2005)

Artificial neural network (ANN) modeling and multiple linear regression (MLR) analysis have been used to develop a powder hard-facing process using high-energy plasma-transferred (HEPT) heating. HEPT heating can produce coatings with minimal surface roughness. An optimal procedure was developed involving the least number of process parameters but producing the most desirable performance characteristic. The quality characteristic of interest is the surface roughness after HEPT processing, utilizing the "the-smaller-the-better" criterion. Process performance was evaluated with respect to the signal-to-noise ratios, which were obtainable through experiments. The experimental results conclude that ANN models demonstrate a greater accuracy of predicting the surface appearance than the MLR models in terms of prediction error and the coefficient of determination. The results also reveal the most significant process control parameters. The predicted value of powder hard-facing roughness, through the implementation of optimal settings, produces a satisfactory result. The confirmation experiment showed that the ANN method achieved the expected optimal design goals for the HEPT powder hard-facing, thereby justifying the reliability and feasibility of the approach.

Keywords artificial neural network, hard-facing, high-energy plasma transfer, multiple linear regression, Taguchi methods

1. Introduction

Powder hard-facing coatings are used frequently to improve surface wear resistance. Surface treatments and coating technologies, including, for example, welding, surface hardening, and thermal spraying, generate hard thick layers on exterior surfaces of heat-resistant or wear-resistant materials. This process produces industrial components with better performance characteristics, such as improved appearance or better protection against corrosion and high temperatures.

Recently, a high-energy plasma-transferred (HEPT) coating process was developed for industrial use, and it has overtaken traditional powder hard-facing techniques such as oxyacetylene and tungsten inert gas welding for surface modification (Ref 1, 2). Surface powder hard-facing by plasma transfer welding plays an important role in the manufacture of aircraft components. Specific functional improvements are attributed to denser packing through efficient microwelding during the powder hard-facing process (Ref 3). Selected micropowdered alloys have been used to solve wear problems due to their high resistance to corrosion, erosion, and cyclic thermal and mechanical stresses (Ref 4-7).

Theoretically, HEPT coatings should produce powder hard-faced microalloys with high strength, hardness, and excellent resistance to wear and corrosion. Unfortunately, this is not true in all cases. Few materials can meet the specific demands by altering their physical and chemical surface properties during hard-facing. Therefore, the characteristics of coating surface topography have been investigated for decades. For example, most research has examined the wear and mechanical properties, corrosion performance, and hard-facing microstructure as a function of coating process (Ref 8, 9). Understanding the characteristics of a hard-faced surface can assist in predicting wear behavior and controlling the extent of wear damage. However, knowledge that can systematically optimize a hard-facing coating is lacking. In particular, plasma transferred arc (PTA) coating process parameters are not well understood. It is essential to produce hard-faced coatings of high quality, and a systematic design process is needed in which process control parameters are known and optimized.

A simple, efficient, and systematic procedure developed by Taguchi (Ref 10) utilizes orthogonal arrays to obtain the best possible model with the fewest experiments. Over the past 15 years, many manufacturers around the world have successfully used this technique, because it allows them to minimize manufacturing time and costs.

Multiple linear regression (MLR) analysis (Ref 11-13) is one of the most widely used statistical techniques. It not only provides simple methods for establishing a functional relationship between the response and explanatory variables, but also gives reasonable predictions of the responses.

Artificial neural network (ANN) modeling (Ref 14) was originally inspired from the operation of the brain. The modeling simulates the learning, clustering, and reasoning capabilities of the brain. Combining such a strong learning capability with parallel computation and nonlinear mapping, ANN modeling has been used to solve nonlinear systems and process control problems (Ref 15-24). To develop a functional model, ANN applies a back-propagation algorithm to train multiple-layered, feed-forward networks using diverse transfer functions. A well-trained ANN model can estimate predictive

Ming-Der Jean, Department of Electrical Engineering, Yung-Ta Institute of Technology & Commerce, 316 Chunshan Rd, Lin-Lo, Ping-Tung, Taiwan 909, Republic of China; **Shu-Yi Tu,** Department of Mathematics, University of Michigan-Flint, Flint, MI 48502; and **Jen-Ting Wang,** Department of Mathematics, Computer Science, and Statistics, State University of New York College at Oneonta, Oneonta, NY. Contact e-mail: mdjeam@mail.ytit.edu.

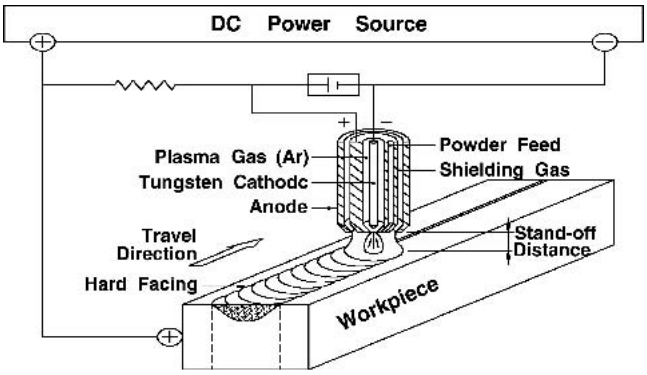

Fig. 1 Powder hard-facing equipment schematic used in the PTA coating

performance through pattern association and pattern classification.

As mentioned above, Taguchi design methodology, MLR analysis, and ANN modeling are effective tools for obtaining good process control; however, their concurrent application has been limited. Therefore, this article proposes a method that combines either ANN or MLR with Taguchi methodology, thereby taking advantage of the strength of each technique to improve the specific engineering design. The proposed approach not only yields sufficient understanding of the effects of the process parameters, but also determines an optimal process route to ensure that the design goals are met, in this case, that the surface morphology of a HEPT powder hard-facing exhibits the best possible performance characteristics.

2. Powder Hard-Facing, High-Energy Plasma-Transferred Coating Process

2.1 Superalloy Hard-Facings

Figure 1 shows the equipment used to produce the powder hard-facing in the HEPT process with the surface ripples of coating layer shown. The hard-facing surface in the coating zone consists of the primary wear-resistant alloy and the melted powder hard-facing in the joined bead.

High-energy plasma-transferred welding is the melting and atomizing of alloy feedstock into a powder using plasma. The process forces gas through an electric arc connecting nonconsumable electrodes in a torch. The plasma is the heat source, forming a molten weld in the same manner as gas tungsten arc welding. When the hard-facing is applied to a surface that can sustain substantial surface buildup, it produces a coating on that material. The HEPT does not penetrate the workpiece thickness as in the hardening process, and it yields a thicker deposit than either thin-film coating or metallic plating. Thus, HEPT hard-facing is best suited for surfaces needing thick deposits. Specifically, this process is appropriate for rebuilding worn parts because it can be applied to almost any substrate using a variety of coating compositions.

2.2 Experimental Setup

The hard-facing materials used in this study are powders with compositions Co-2.4wt.%C-0.1wt.%Mo-1.1wt.%Si-12.5wt.%W-30wt.%Cr and Ni-0.45wt.%C-2.9wt.%Fe-3.9wt.%Si-0.05wt.%B-11wt.%Cr with particles ranging from 40 to 70 μm. These superalloy powders are specifically used in surface-engineering applications. In the HEPT coating experiments, the powders were deposited onto SKD61 tool steel using the PTA coating process. The Co-base powder is widely applied to wear-resistant components, while the Ni-base powder is used for heat-resistant and corrosion-resistant hard-facings. Due to limitations of the machining equipment and manufacturing setup for the HEPT process, control factors were selected as shown in Table 2. The selection criteria were based on data in HEPT technical reports and opinions from welding experts (Ref 6).

Table 1 Control factors and their levels

	Process control factor	Level 1	Level 2	Level 3
A	Powder hard-facing type	Co-base	Ni-base	…
B	Accelerating voltage, V	10	15	25
C	Electric arc current, A	100	130	160
D	Travel speed, cm/min	6	10	15
E	Torch standoff, mm	8	12	15
F	Powder feed rate, L/min	3	4.5	6
G	Pilot gas flow rate, L/min	2.5	3.0	3.5
H	Preheat treatment, °C	25	150	250

An optical microscopy and surface profilometry were used to measure the roughness dimensions and the mean surface roughness (R_a) of the hard-facing to select the best morphology of the bead surface over the 2.4 mm length. The laser gage was used to scan the surface topography, and the image of the geometric figure was reproduced as a plane of the hard-facing bead over a 1 mm^2 area.

3. Statistical Design of Experiment

3.1 Taguchi Design

The Taguchi method provides a simple, efficient, and economic approach to estimating quality characteristics as well as reducing costs. This method utilizes orthogonal arrays to give a systematic evaluation for the process design factors of interest. The orthogonal arrays are intentionally designed to collect sufficient information while using the least number of experiments. In Table 1, the eight control factors used in the design matrix are shown with the level of significance for each HEPT hard-facing control factor. To be specific, the control factors included: the type of hard-facing alloy powder; the accelerating voltage; the electric arc current; the electric arc speed of travel; the stand-off torch distance; the powder feed rate; the flow rate of the pilot gas; and the preheat temperature.

Table 2 presents the experimental layout for the L_{18} orthogonal array. Except for factor A, which has only two levels, the other seven factors have three levels. Therefore, $2^1 \times 3^7$ experiments are needed to produce a full factorial design experiment, but only 18 are needed for the L_{18} orthogonal array.

3.2 Evaluation of the Signal-to-Noise Ratio

The formulation of the signal-to-noise ratio (SNR) is designed so that a larger value leads to better process results. However, the method for calculating SNR varies and depends on whether the response variable is too large, too small, or on target. In this case, the SNR formula follows the-smaller-the-better criterion because the response variable (i.e., surface

Table 2 Experimental results

Test	PTA control factors								Coating surface roughness (R_a)					SNR, dB
	A	B	C	D	E	F	G	H	N1, μm	N2, μm	N3, μm	Mean	SD	
1	1	1	1	1	1	1	1	1	9.8	10.3	11.1	10.40	0.66	−20.35
2	1	1	2	2	2	2	2	2	12.4	13.1	12.7	12.73	0.35	−22.10
3	1	1	3	3	3	3	3	3	11.1	13.1	10.6	11.60	1.32	−21.33
4	1	2	1	1	2	2	3	3	14.4	17.1	15.6	15.70	1.35	−23.94
5	1	2	2	2	3	3	1	1	18.6	21.2	20.1	19.97	1.31	−26.02
6	1	2	3	3	1	1	2	2	11.2	11.3	10.7	11.07	0.32	−20.88
7	1	3	1	2	1	3	2	3	14.1	14.2	14.3	14.20	0.10	−23.05
8	1	3	2	3	2	1	3	1	11.4	11.5	12.1	11.67	0.38	−21.34
9	1	3	3	1	3	2	1	2	14.3	14.7	15.1	14.70	0.40	−23.35
10	2	1	1	3	3	2	2	1	13.9	15.9	14.9	14.90	1.00	−23.48
11	2	1	2	1	1	3	3	2	17.1	18.3	19.8	18.40	1.35	−25.31
12	2	1	3	2	2	1	1	3	16.7	17.4	19.1	17.73	1.23	−24.99
13	2	2	1	2	3	1	3	2	11.3	10.7	11.1	11.03	0.31	−20.86
14	2	2	2	3	1	2	1	3	17.1	15.6	17.5	16.73	1.00	−24.48
15	2	2	3	1	2	3	2	1	13.9	12.1	11.7	12.57	1.17	−22.01
16	2	3	1	3	2	3	1	2	13.4	14.2	15.6	14.40	1.11	−23.18
17	2	3	2	1	3	1	2	3	13.1	12.6	12.9	12.87	0.25	−22.19
18	2	3	3	2	1	2	3	1	12.6	13.2	13.8	13.20	0.60	−22.42
19	1	3	1	3	1	1	2	1	8.5	8.5	8.7	8.57	0.13	−18.66

A, powder hard-facing type; B, accelerating voltage, V; C, electric arc current, A; D, travel speed, cm/min; E, torch standoff, mm; F, powder feed rate, L/min; G, pilot gas flow rate, L/min; H, preheat treatment, °C; SD, standard deviation; SNF, signal-to-noise ratio

Table 3 The signal-to-noise ratios for control factors and levels

	A	B	C	D	E	F	G	H
Level 1	−22.49	−22.93	−22.48	−22.87	−22.75	−21.77	−23.73	−22.61
Level 2	−23.22	−23.04	−23.58	−23.24	−22.93	−23.30	−22.29	−22.62
Level 3	…	−22.59	−22.50	−22.46	−22.88	−23.49	−22.54	−23.34
Effect	0.73	0.45	1.10	0.78	0.18	1.72	1.45	0.73
Rank	5	7	3	4	8	1	2	6

roughness) is to be as small as possible. The Taguchi SNR formula takes both the average and the standard deviation into consideration:

$$SNR_i = -10\log\left[\frac{1}{n}\sum_{j=1}^{n} Y_{ij}^2\right] \quad \text{(Eq 1)}$$

where SNR_i stands for the SNR of the i^{th} test, n is the total number of trials in each test, and Y_{ij} denotes the observed surface roughness of the j^{th} trial for the i^{th} test. More precisely, two repeated trials are performed for each of the 18 hard-facing tests, so $n = 3$ and i ranges from 1 to 18.

3.3 Analysis of Variance

To determine how the control factors affect the surface roughness, analysis of variance (ANOVA) is performed, which estimates and tests the effects of different treatments on the response variable. Based on the analysis, the factors that have the most significant effect on surface roughness are determined. Subsequent experiments can be focused on these factors during HEPT coating. The ANOVA table contains variations (i.e., sums of squares) of the process control factors as well as random errors, degrees of freedom, mean squares, *F*-values, and contribution percentages. The contribution percentage is used to compare the relative importance of contributions from the process control factors. Factors with higher contribution percentages are ranked higher in terms of importance in the experiment. That is, they have a significant effect on the quality criterion.

3.4 Multiple Linear Regression Analysis

Multiple linear regression analysis is a procedure that predicts a dependent/response variable from two or more independent variables using a linear function. To determine the best fit to the data, the least-squares method is used to minimize the sum of all squared deviations from the predicted results and the actual data. With a sample of n observations of the dependent variable Y, a possible MLR model with interaction effects takes the form (Ref 12):

$$Y_i = \beta_0 + \sum_{j=1}^{p-1}\beta_j X_{ij} + \sum_{\substack{j,k=1 \\ j\neq k}}^{p-1}\beta_{jk} X_{ij} X_{ik} + \varepsilon_i, \quad i = 1, \ldots, n \quad \text{(Eq 2)}$$

where Y_i stands for the ith observation of Y, X_{ij} denotes the ith observation of the jth independent variable, and β's are the unknown regression parameters to be determined. The random errors ε_i are assumed to be independent from one another, and follow a normal distribution with a mean of zero and a constant variance of σ^2.

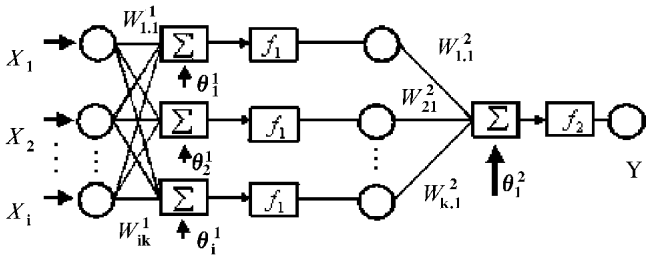

Fig. 2 Structure of the three-layer ANN

3.5 Artificial Neural Network

The back-propagation algorithm first proposed by Werbos (Ref 13) in the 1970s is the most widely used ANN. When a back-propagation network is cycled, the activations of the input nodes are propagated forward to the output layer through the connecting weights. The idea of network construction is shown in Fig. 2. In this study, a network is needed for eight signal inputs and one output. Therefore, (X_1, X_2, . . . , X_8), (H_1, H_2, . . . , H_n), and Y are the inputs, hidden-layer outputs, and output-layer outputs, respectively, where the output of each hidden-layer node is:

$$H_k = f_1\left(X_1, X_2, \ldots, X_8\right) = \left[1 + \exp\left(-\sum_{i=1}^{8} W^1_{ik} \cdot X_i + \theta^1_i\right)\right]^{-1}, k = 1, \ldots, n \quad \text{(Eq 3)}$$

and the output of the output-layer is

$$Y = f_2(H_1, H_2, \ldots, H_n) = \left[\sum_{k=1}^{n} W^2_{k1} \cdot H_k + \theta^2_k\right] \quad \text{(Eq 4)}$$

f_1 and f_2 denote the transfer functions for the hidden and output layers, respectively. As seen in Eq 3 and 4, the activation function f_1 is a logistic sigmoid transfer function in [0, 1], and f_2 is a linear function. W^1_{ik} represents the connection weight from the i^{th} input node to the k^{th} hidden node, and W^1_{k1} represents the connection weight from the i^{th} hidden-layer node to the output. The θ values denote the biases between nodes. The selection for the training of the network is the steepest gradient descent algorithm, which should converge to the desired value. The ANN training is carried out until the cost function (i.e., the error between the output response value and the target value) is within a desired value.

4. Experimental Results and Discussion

4.1 Analysis of the Experimental Results

The quality characteristic for the HEPT powder hard-facing process is the local surface roughness of the hard-facing zone. Table 2 shows the experimental surface roughness results. Among the 18 experimental trials, test 1 had the smallest mean surface roughness (10.40 μm), while Test 5 had the largest mean roughness (19.97 μm). It is evident that the specimens had much larger surface roughness values compared with those of the parent material (6 to 7 μm), because HEPT powder hard-facing yields a dense thick deposit. This is attributed to the heat-flow motion of the powered alloys in the areas of the molten substrate.

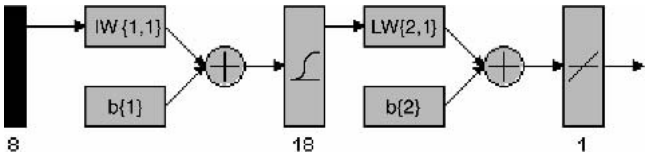

Fig. 3 The trained 8-18-1 ANN structure

Table 4 Analysis of variance for Taguchi methods

Source of variation	Sum of squares	Degrees of freedom	Variance	Variance ratio	Percentage contribution
A	2.803	1	2.803	17.786	6.108
B	0.966	2	0.483	3.064	2.105
C	7.111	2	3.555	22.560	15.496
D	4.784	2	2.392	15.179	10.426
E	0.150	2	0.075	0.476	0.327
F	15.899	2	7.949	50.440	34.646
G	10.745	2	5.373	34.089	23.415
H	3.116	2	1.558	9.886	6.790
Error	0.315	2	0.158	12.690	0.687
Total	45.889	17	2.699	6.298	100.00

A, powder hard-facing type; B, accelerating voltage, V; C, electric arc current, A; D, travel speed, cm/min; E, torch standoff, mm; F, powder feed rate, L/min; G, pilot gas flow rate, L/min; H, preheat treatment, °C

4.2 The Signal-to-Noise Response Effects and the Optimal Setting

The performances of the experimental settings are evaluated from the SNR (Table 2). The SNR response effects in Table 3 show the differences of the largest-level SNR and the smallest-level SNR for each of the factors. Factors F-powder feed rate, G-pilot gas flow rate, C-electric arc current, and D-arc travel speed have relatively strong effects on the variability in powder hard-facings roughness. The SNR response effect analysis also identified the optimal experimental conditions (i.e., the largest SNR for each factor) for the HEPT hard-facing process: A1; B3; C1; D3; E1; F1; G2; and H1.

4.3 Analysis of Variance for Taguchi Methods

The ANOVA was used to evaluate the significances of various factors affecting surface roughness. The ANOVA for the experimental SNR results is shown in Table 4. It is clear that factors F, G, C, and D (decreasing order of importance) are the most significant processing parameters and coincide with the conclusions drawn from Table 3. These factors account for nearly 84% of the total variance of roughness.

4.4 The Multiple Linear Regression Analysis

The control factors are selected as the independent variables and the second-order interactions of the four most significant

factors (C, D, F, and G) as obtained in section 4.3 to establish the MLR model. The least-squares regression equation is:

$$\hat{Y} = -38.86 + 2.17A + 0.19B + 0.56C - 0.64D + 0.42E - 4.89F + 18.26G - 0.022H + 0.02CD - 0.03CF - 0.22CG - 0.01DF - 0.79DG + 3.43FG \quad \text{(Eq 5)}$$

The correlation coefficient (R^2) is 0.744 for Eq 5, indicating that approximately 74% of the total variance of the surface roughness can be accounted for by the eight control factors. For comparison, other MLR models are compared with the ANN model in section 4.6.

4.5 The Artificial Neural Network Simulation of High-Energy Plasma-Transferred Powder Hard-Facing Process

It has been shown by theoretical studies that one hidden layer, coupled with logistic sigmoid transfer function, will be sufficient for ANN structures (Ref 8). The numerical relations between the number of training patterns and input variables usually play an important role in determining the number of nodes in hidden layers, which is considered to be a matter of great significance due to its effect on the error function. A single hidden-layer ANN is denoted by *i-k-j* with *i* inputs, *j* outputs, and *k* as the number of nodes in the hidden layer. The ANN models used herein are 8-18-1 and 4-18-1 networks. Figure 3 shows the diagram for the trained optimal 8-18-1 ANN structure in which the error function in learning iterations is bounded within the desired value. For both structures, the powder hard-facing roughness is the output response. However, the input signal for the 8-18-1 model possesses eight control factors, while the 4-18-1 model uses the four significant control factors determined from the ANOVA. The learning process is iterative with the training set propagating to ANN repeatedly until the error function reaches the desired value. Figures 4 and 5 show the convergence of the root mean square (RMS) values of the two models from the trained data. As shown in these figures, the RMS of the trained ANN has reduced to a pleasing value of 10^{-27} μm after <5500 training epochs. (In this article, the ANN models train 10^4 epochs.) The 8-18-1 and 4-18-1 ANN models yield almost the same result. However, the 4-18-1 ANN model achieves the same desired RMS error in fewer iterations than the 8-18-1 ANN model. The interconnection weights-*IW*(1,1) and *LW*(1,2) and biases-*b*(1) and *b*(2) in the trained networks are determined when the RMS error is minimized. The adjusted weights using the steepest gradient method are shown in Table 5.

4.6 Comparative Analyses of Artificial Neural Network and Multiple Linear Regression

Table 6 shows the results from various models using the MLR and ANN methods. The MLR models with more explanatory variables yield better fits and predictions. In Table 6, model 3 (equivalent to Eq 5) is the best model, yielding a moderate fit with $R^2 = 0.7442$ and a mean prediction error of 1.145 μm.

Table 5 The adjusted weights of the 8-18-1 artificial neural network (ANN) model

$$IW(1,1) = \begin{bmatrix} 0.39127 & 0.43978 & 2.9327 & 0.064149 & 0.02418 & 1.577 & 4.0716 & 4.0919 \\ -4.0277 & -0.58133 & -3.431 & -0.31437 & 0.52434 & 0.054155 & -2.002 & -0.70446 \\ -4.518 & 19.1691 & 0.95517 & -18.5625 & 10.0141 & 1.3671 & -3.721 & -0.20266 \\ -2.5689 & -0.095383 & -0.17542 & -0.16771 & 0.67896 & 0.36032 & 4.8564 & -0.074196 \\ -0.083534 & -17.2497 & -3.727 & -9.2687 & -0.86813 & 2.5315 & -3.8087 & 1.7605 \\ -0.14848 & -0.24318 & -0.0089413 & 0.19587 & -0.422681 & 1.3551 & 3.4972 & 0.50924 \\ 4.4112 & -0.24318 & 0.1532 & -0.20757 & -0.21003 & -0.99199 & 2.1793 & 0.14336 \\ 1.0976 & -0.28883 & 0.13995 & -0.16096 & -0.60647 & 1.5457 & 4.8552 & -0.036122 \\ -1.7981 & 0.36381 & 0.088325 & -0.048089 & 0.48659 & 0.083271 & -3.0517 & 0.088608 \\ 15.6074 & 1.9004 & -0.49745 & 2.1681 & -2.2735 & 14.5015 & -21.6521 & 0.22946 \\ 1.2582 & -2.0682 & -11.3218 & -1.0612 & -0.50743 & 0.66539 & -4.2057 & -2.1156 \\ -3.4286 & 0.28551 & 1.0194 & 0.32948 & -0.03261 & -0.87665 & 3.595 & 0.22894 \\ 3.1586 & 16.6337 & -7.0953 & 23.6581 & -8.8894 & -7.602 & -0.37002 & 5.6206 \\ 5.2207 & 0.023976 & 0.22091 & -0.39909 & -0.58224 & -1.0848 & -1.8422 & -1.1135 \\ 0.9243 & 0.27778 & -0.22479 & -0.26889 & -0.26494 & 1.5074 & -1.2178 & -0.10729 \\ -4.2033 & -0.13017 & 1.3451 & 0.66553 & 0.32592 & -0.34628 & 3.166 & -4.7486 \\ 2.5366 & 3.9058 & -0.27783 & -8.2523 & 3.3664 & -1.5823 & -1.6594 & 0.28458 \\ 0.67689 & 0.2809 & -1.1619 & 2.0091 & 0.50135 & -0.063662 & -3.8055 & 1.5319 \end{bmatrix}$$

$$LW(2,1) = \begin{bmatrix} -0.94186 & -0.35754 & -2.6154 & -0.55355 & -0.69749 & -0.46708 & 2.2161 & 3.0311 \\ 2.4188 & 14.1385 & -0.58619 & 1.0555 & -11.8543 & -3.0654 & 0.65123 & 5.494 \\ 6.7976 & -0.13802 & & & & & & \end{bmatrix}$$

$$b(1) = \begin{bmatrix} -0.60 & 17.16 & 35.01 & -7.37 & 3.39 & 2.87 & -1.97 & -20.52 \\ 17.93 & -6.84 & 21.65 & -13.89 & 0.12 & 7.361 & -2.11 & -21.81 \\ 12.70 & 5.57 & & & & & & \end{bmatrix}$$

$$b(2) = [2.14]$$

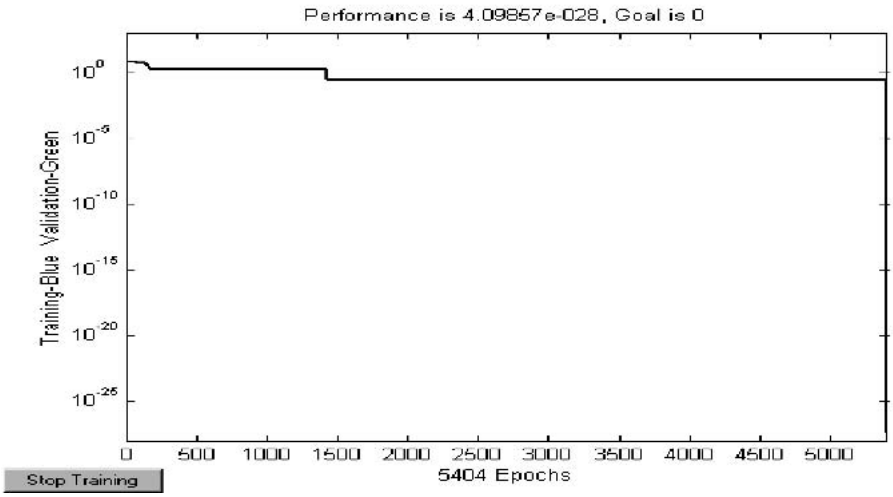

Fig. 4 The RMS error performance of the 8-18-1 ANN model

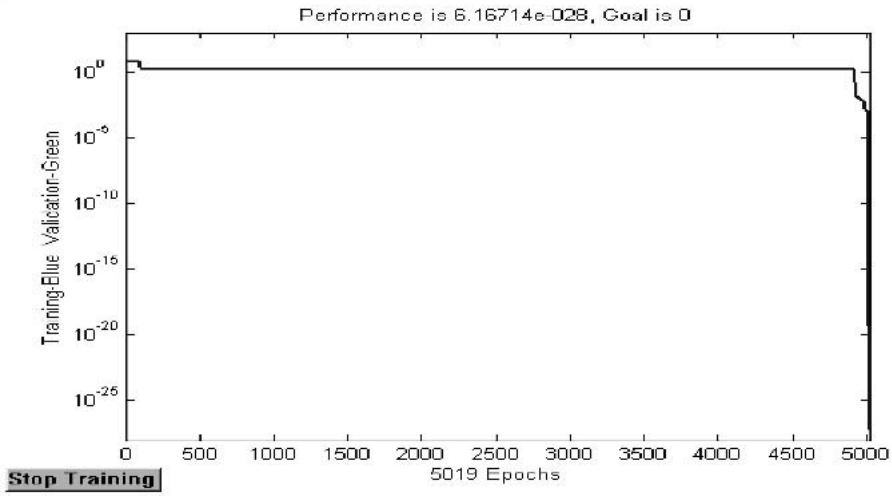

Fig. 5 The RMS error performance of the 4-18-1 ANN model

Table 6 Performance statistics between multiple linear regression and artificial neural network models

		Multiple linear regression (MLR)		Artificial neural network (ANN)	
Model	**Control factor combination**	R^2	**Average error**	R^2	**Average error**
1	A, B, C, D, E, F, G, H	0.37	1.782	0.9999	1.42×10^{-14}
2	A, B, C, D, E, F, G, H, CD, CF, CG, DF and DG	0.74	1.145	…	…
3	C, D, F, G	0.29	1.875	0.9999	9.95×10^{-13}
4	C, D, F, G, CD, CF, CG, DF, DG	0.60	1.375	…	…

A, powder hard-facing type; B, accelerating voltage, V; C, electric arc current, A; D, travel speed, cm/min; E, torch standoff, mm; F, powder feed rate, L/min; G, pilot gas flow rate, L/min; H, preheat treatment, °C

Note that in the ANN models, a nonlinear activation function (Eq 3) is used to transform the input variables, incorporating the interactions among them. Hence, it is not necessary to add interaction terms in the ANN models. The 4-18-1 ANN model with variables C, D, F, and G makes predictions as accurate as the full ANN model with all control factors. The mean prediction error for the 4-18-1 ANN model is 9.95×10^{-13} μm, while it is 1.42×10^{-14} μm for the 8-18-1 ANN model. Both models yield nearly perfect correlations with $R^2 = 0.9999$.

In light of the above comparisons, both ANN models yield higher accuracy than the MLR models. The ANN model with only four input variables produces better fits and predictions than the more complex MLR models.

4.7 Hard-Facing Appearance Examination Analysis

Figures 6 and 7 show images of the three-dimensional laser hard-facing surface with associated statistics for test 18, the optimal trial. Compared with the average spacing between

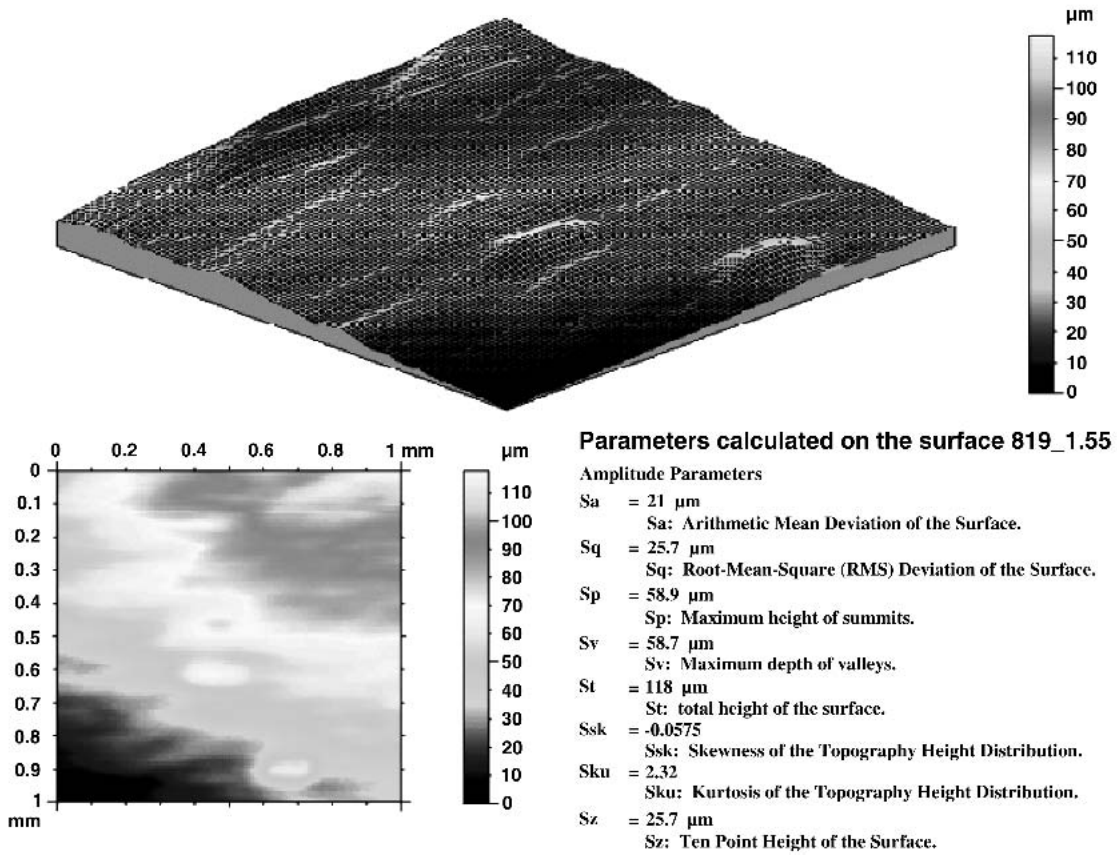

Fig. 6 Three-dimensional laser photograph of powdered hard-facing layers for test 18

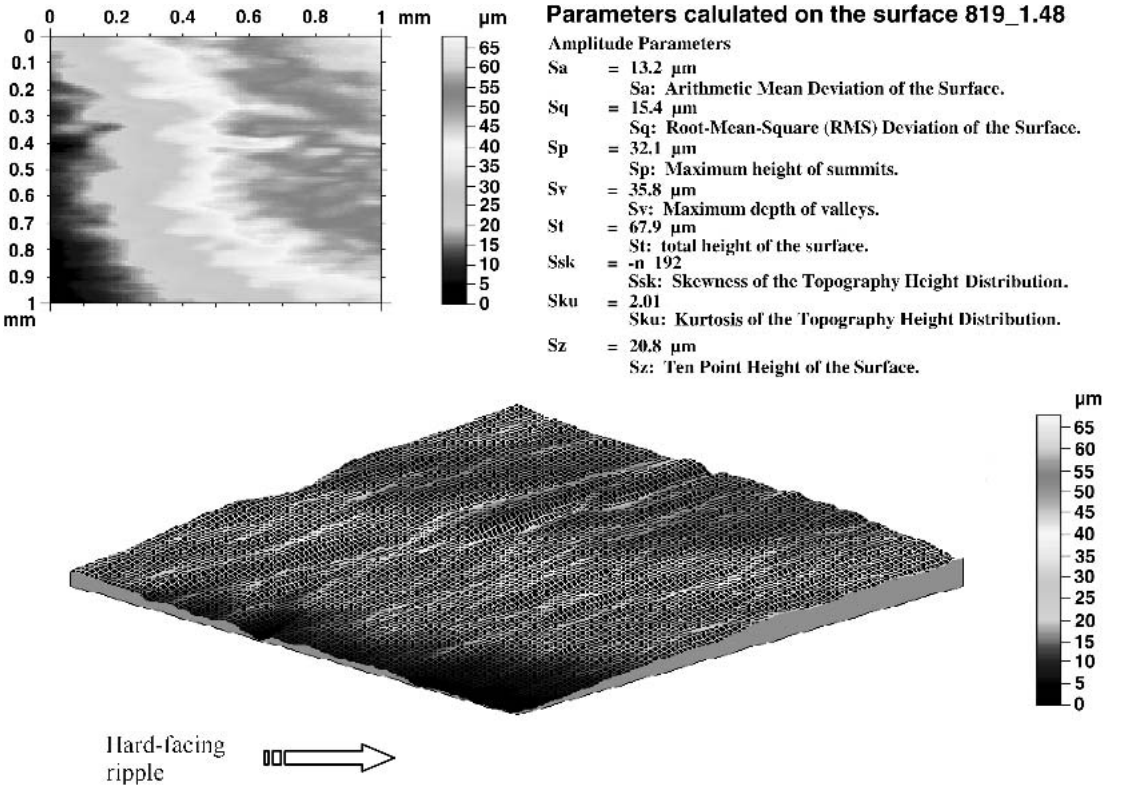

Fig. 7 Laser three-dimensional photograph of powered hard-facing layers for the optimal setting

coarse ripples of 4.94 mm from the original 18 trials, the optimal trial produces a wider surface spacing of 10.36 mm. It yields an arithmetic mean deviation of hard-facing surface of 13.2 μm and a surface roughness value of 8.57 μm. The appearance of the surface beads also reveals that the optimal trial produces a smoother hard-facing surface. Because surface tension drives the liquid flowing under the arc beam at the surface, the movement of the flowing liquid is balanced by an equal and opposite flow beneath the hard-facing. The optimal setting produces a maximum height of the summits equal to 32.1 μm, and a maximum depth of valleys equal to 35.8 μm. It is evident that the appearance of the hard-faced surface using the optimal process control settings results in a finer ripple compared with the other tests. Thus, the optimal setting should produce better hard-facing surfaces, with reduced postprocess machine working time and cost.

The ripples in the powder hard-faced surface are produced as a result of a variation in liquid flow to the back edge of the coating pool as a consequence of convection and evaporation effects. During the HEPT coating process, the matrix substrate partially melts, and then rapidly solidifies as a self-quenching hard-facing layer. It is because the coating layers rapidly cool that they can be used for wear, heat, and corrosion resistance. Thus, it is worth noting that the surface produced using the optimal setting is better than those obtained with the other process control settings.

5. Conclusions

Comparisons using ANN and MLR models for process control in HEPT powder hard-facing operations for wear-resistant surfaces on tool steel have been described. Based on the experimental results:

1) Using the Taguchi method, the most significant factors affecting the hard-facing surface roughness are electric arc current, speed of travel, powder feed rate, and rate of gas flow.
2) The following factors yield the best combination of process variables:
   - Factor A, level 1; factor B, level 3; factor C, level 1; factor D, level 3;
   - Factor E, level 1; factor F, level 1; factor G, level 2; factor H, level 1.
3) Photographic examination of the hard-facing morphology for HEPT coatings shows minor hard-faced roughness due to surface tension. This occurred because the liquid that flowed under the arc at the surface was balanced by flow beneath the powder hard-facing.
4) The ANN models train and learn HEPT powder hard-facings well. The simple ANN model using the four most significant control variables produces a prediction as accurate as the full ANN model. The mean prediction errors for the simple and complete ANN models are 9.95×10^{-13} μm and 1.42×10^{-14} μm, respectively. Both models yield nearly perfect correlation ($R^2 = 0.999$).
5) The ANN models generally demonstrate greater accuracy in predicting powder hard-facing roughness for HEPT-coated substrate than MLR models. The best MLR model (Eq 5) yields a lower correlation ($R^2 = 0.744$) and a larger average error (1.145 μm) than the ANN models.

References

1. R.V. Sharples, *The Plasma Transferred Arc Weld Surfacing Process,* The Welding Institute, 1985
2. K.M. Kuldarni and V. Anand, Metal Powders Used for Hard-facing, *Metals Handbook,* 9th ed., ASM International, 1981
3. G. Kenneth, *Surface Engineering for Wear Resistance,* Prentice Hall, Englewood Cliffs, NJ, 1988
4. K.Y. Lee, S.H. Lee, Y. Kim, H.S. Hong, Y.M. Oh, and S.J. Kim, The Effects of Additive Elements on the Sliding Wear Behavior of Fe-base Hard-Facing Alloys, *Wear,* Vol 255, 2003, p 481-488
5. J.N. Aoh and J.C. Chen, On the Wear Characteristics of Cobalt-based Hard-facing Layer after Thermal Fatigue and Oxidation, *Wear,* Vol 250, 2001, p 611-620
6. R.G. Bayer, *Wear Analysis for Engineers,* HNB Publishing, New York, 2002
7. A.S.C.M. d'Oliveira, R. Vilar, and C.G. Feder, High Temperature Behavior of Plasma Transferred Arc and Laser Co-based Alloy Coatings, *Appl. Surf. Sci.,* Vol 201, 2002, p 154-160
8. W. Schwarz, and H. Warlimont, A New Series of Co-based Amorphous Alloys and Their Application as Cladding Materials, *Mater. Sci. Eng., A,* Vol 226-228, 1997, p 1098-1101
9. J.C. Shin, J.M. Doh, J.K. Yoon, D.Y. Lee, and J.S. Kim, Effect of Molybdenum on The Microstructure and Wear Resistance of Cobalt-base Stellite Hard-facing Alloys, *Surf. Coat. Technol.,* Vol 166, 2003, p 117-126
10. W. Yuin and W. Alan, *Taguchi Methods for Robust Design,* ASME, 2000
11. J. Devore, and N. Farnum, *Applied Statistics for Engineers and Scientists,* International Thomson, 1999
12. J. Rawlings, *Applied Regression Analysis,* Springer-Verlag, New York, 1998
13. P.J. Werbos, Back propagation through time: What it is and how to do it, *Proceedings of the IEEE,* Vol 78, 1990, p 1550-1560
14. C.T. Lin and C.S. Lee, *Neural Fuzzy Systems: A Neuro-Fuzzy Synergism to Intelligent Systems,* Prentice Hall, Simon & Schuster, 1996
15. L.N. Smith, R.M. German and M.L. Smith, A Neural Network Approach for Solution of the Inverse Problem for Selection of Powder Metallurgy Materials, *J. Mater. Proc. Technol.,* Vol 120, 2002, p 419-425
16. I.S. Kim, J.S. Son, C.E. Park, C.W. Lee, K. Yarlagadda, and D.V. Prasad, A Study on Prediction of Bead Height in Robotic Arc Welding Using a Neural Network, *J. Mater. Proc. Technol.,* Vol 130-131, 2002, p 229-234
17. M. Hur, T.H. Hwang, W.T. Ju, C.M. Lee, and S.H. Hong, Numerical Analysis and Experiments on Transferred Plasma Torches for Finding Appropriate Operating Conditions and Electrode Configuration for a Waste Melting Process, *Thin Solid Films,* Vol 390, 2001, p 186-191
18. R.K. Jain, V.K. Jain, and P.K. Kalra, Modelling of Abrasive Flow Machining Process: a Neural Network Approach, *Wear,* Vol 231, 1999, p 242-248
19. M, Vijaya, R. Krishna, O. Prabhakar, and N.G. Shankar, Simultaneous Optimization of Flame Spraying Process Parameters for High Quality Molybdenum Coatings Using Taguchi Methods, *Surf. Coat. Technol.,* Vol 79, 1996, p 276-288
20. L.J. Yang, Plasma Surface Hardening of ASSAB 760 Steel Specimens with Taguchi Optimization of the Processing Parameters, *J. Mater. Proc. Technol.,* Vol 113, 2001, p 521-526
21. T.A. Theodore and G.P. Maul, A Method for Robust Process Design Based on Direct Minimization of Expected Loss Applied to Arc Welding, *J. Manuf. Systems,* Vol 20, 2001, p 329-348
22. Z. Zhang, N.M. Barkoula, J. Karger-Kocsis, and K. Frisdrich, Artificial Neural Networks Predictions on Erosive Wear of Polymers, *Wear,* Vol 255, 2003, p 708-713
23. D.S. Nagesh and G.L. Datta, Prediction of Weld Bead Geometry and Penetration in Shielded Metal-Arc Welding Using Artificial Neural Networks, *J. Mater. Proc. Technol.,* Vol 123, 2002, p 303-312
24. R.K. Ohdar and S. Pasha, Prediction of the Process Parameters of Metal Powder Perform Forging Using Artificial Neural Network, *J. Mater. Proc. Technol.,* Vol 132, 2003, p 227-234